ELSEVIER

Contents lists available at ScienceDirect

Computers and Mathematics with Applications

www.elsevier.com/locate/camwa



A Carleman-based numerical method for quasilinear elliptic equations with over-determined boundary data and applications



Thuy T. Le^a, Loc H. Nguyen^{a,*}, Hung V. Tran^b

- ^a Department of Mathematics and Statistics, University of North Carolina at Charlotte, Charlotte, NC, 28223, USA
- b Department of Mathematics, University of Wisconsin-Madison, Madison, WI, 53706, USA

ARTICLE INFO

Keywords: Carleman estimate Linearization Boundary value problems Quasilinear elliptic equations Hamilton-Jacobi equations Inverse problems

ABSTRACT

We propose a new iterative scheme to compute the numerical solution to an over-determined boundary value problem for a general quasilinear elliptic PDE. The main idea is to repeatedly solve its linearization by using the quasi-reversibility method with a suitable Carleman weight function. The presence of the Carleman weight function allows us to employ a Carleman estimate to prove the convergence of the sequence generated by the iterative scheme above to the desired solution. The convergence of the iteration is fast at an exponential rate without the need of an initial good guess. We apply this method to compute solutions to some general quasilinear elliptic equations and a large class of first-order Hamilton-Jacobi equations. Numerical results are presented.

1. Introduction

The main aim of this paper is to develop a numerical method based on Carleman estimates to solve quasilinear elliptic PDEs with overdetermined boundary data. We consider this new method as the second generation of Carleman-based numerical methods while the first generation is called the convexification, which will be mentioned in detail later. Let Ω be an open and bounded domain in \mathbb{R}^d , $d \geq 2$, with smooth boundary $\partial \Omega$. Let f and g be two smooth functions defined on $\partial \Omega$. Let $F: \overline{\Omega} \times \mathbb{R} \times \mathbb{R}^d \to \mathbb{R}$ be a function in the class C^2 . Let $A = (a_{ij})_{i,j=1}^d : \overline{\Omega} \to \mathbb{R}^{d \times d}$ be C^2 , symmetric, and positive definite, that is,

$$\gamma |\xi|^2 \le a_{ij}(\mathbf{x})\xi_i\xi_j \le \gamma^{-1}|\xi|^2$$
 for all $\mathbf{x} \in \overline{\Omega}$, $\xi \in \mathbb{R}^d$,

for some fixed $\gamma \in (0,1)$. The following problem is of our interests.

Problem 1. Assume that the over-determined boundary value problem

$$\begin{cases}
-\operatorname{div}(A(\mathbf{x})\nabla u(\mathbf{x})) + F(\mathbf{x}, u(\mathbf{x}), \nabla u(\mathbf{x})) = 0 & \mathbf{x} \in \Omega, \\
u(\mathbf{x}) = f(\mathbf{x}) & \mathbf{x} \in \partial \Omega, \\
\partial_{\nu} u(\mathbf{x}) = g(\mathbf{x}) & \mathbf{x} \in \partial \Omega
\end{cases}$$
(1)

has a solution u^* in $C^2(\overline{\Omega})$. Compute the function u^* .

Problem 1 is motivated by a class of nonlinear inverse problems in PDEs, in which f and g are the data that can be measured. One important goal of inverse problems is to reconstruct the internal structure

A natural approach to solve (1) is based on optimization. That means one sets the computed solution to (1) as a minimizer of a mismatch functional, e.g.,

$$v\mapsto J(v):=\int\limits_{\Omega}\Big|-\operatorname{div}(A(\mathbf{x})\nabla v(\mathbf{x}))+F(\mathbf{x},v(\mathbf{x}),\nabla v(\mathbf{x}))\Big|^2\,d\mathbf{x}$$

+ a regularization term

E-mail address: loc.nguyen@uncc.edu (L.H. Nguyen).

https://doi.org/10.1016/j.camwa.2022.08.032

Received 22 April 2022; Accepted 21 August 2022

of a domain from boundary measurements, which allow us to impose both Dirichlet and Neumann data of the unknown in (1). Recently, a unified framework to solve such inverse problems was developed by the research group of the first and second authors, which has two main steps. In the first step, by introducing a change of variables, one derives a PDE of the form (1) from the given inverse problem, in which f and g can be computed directly by the given boundary data. In the second step, one numerically solves (1) to find u^* . The knowledge of u^* directly yields that of the solution to the corresponding inverse problem under consideration. See [1,2] and the references therein for some works in this framework. Moreover, this unified framework was successfully tested with experimental data in [3-5]. Another motivation to study Problem 1 is to seek solutions to Hamilton-Jacobi equations under the circumstance that the Neumann data of the unknown can be computed by its Dirichlet data and the given form of the Hamiltonian, see e.g., [6, Assumption 1.1 and Remark 1.1]. Since inverse problems are out of the scope of this paper, we only focus on the applications in solving quasilinear elliptic PDEs and first-order Hamilton-Jacobi equations.

^{*} Corresponding author.

subject to the Cauchy boundary conditions $v|_{\partial\Omega}=f$ and $\partial_v v|_{\partial\Omega}=g$. The methods based on optimization are widely used in the scientific community, especially in computational mathematics, physics and engineering. Although effective and popular, the optimization-based approaches have some drawbacks:

- 1. In general, it is not clear that the obtained minimizer approximates the true solution to (1).
- The mismatch functional J is not convex, and it might have multiple minima and ravines (see an example in [7] for illustration).
 To deliver reliable numerical solutions, one must know some good initial guesses of the true solutions.
- 3. The computation is expensive and time consuming.

Drawbacks # 1 and #2 can be treated by the convexification method, which is designed to globalize the optimization methods. The main idea of the convexification method is to employ some suitable Carleman weight functions to convexify the mismatch functionals. The convexity of weighted mismatch functionals is rigorously proved by Carleman estimates. Several versions of the convexification method have been developed in [8,1,9–11,5] since it was first introduced in [12]. Moreover, we recently discovered that the convexification method can be used to solve a large class of first-order Hamilton-Jacobi equations [6].

In this paper, we introduce a new method to solve (1) based on linearization and Carleman estimates. Like the convexification method, our method delivers a reliable solution to (1) without requiring a good initial guess. This fact is rigorously proved. Unlike the convexification method which is time consuming, our new method quickly provides the desired solutions. Its convergence rate is $O(\theta^n)$ as $n \to \infty$ for some $\theta \in (0,1)$.

We find the numerical solution to (1) by repeatedly solving the linearization of (1) by a new "Carleman weighted" quasi-reversibility method. The classical quasi-reversibility method was first proposed in [13], and it has been studied intensively since then (see [14] for a survey). By a Carleman weighted quasi-reversibility method, we mean that we let a suitable Carleman weight function involve in the cost functional suggested by the classical quasi-reversibility method. The presence of the Carleman weight function is the key for us to prove our convergence theorem. Our process to solve Problem 1 is as follows. We first choose any initial solution that might be far away from the true one. Denote this initial solution by the function u_0 . Linearizing (1) about u_0 , we obtain a linear PDE. We then solve this linear PDE by the Carleman weighted quasi-reversibility method to obtain an updated solution u_1 . Using the Carleman weighted quasi-reversibility method rather than the classical one in this step is the key to our success. By iteration, we repeat this step to construct a sequence $\{u_n\}_{n\geq 0}$. The convergence of this sequence to the true solution to (1) is proved by using Carleman estimates. We then apply this method to numerically solve some quasilinear elliptic equations. It is important to note that our approach works well for systems of quasilinear elliptic PDEs too.

Remark 1. In general, (1) is over-determined and it might have no solution, especially when the boundary data contains some noise. Our iteration and linearization method using the Carleman weighted quasi-reversibility method in each step still delivers a function that "most fits" (1).

On the other hand, (1) with only Dirichlet boundary condition, that is, the equation

$$\begin{cases}
-\operatorname{div}(A(\mathbf{x})\nabla u(\mathbf{x})) + F(\mathbf{x}, u(\mathbf{x}), \nabla u(\mathbf{x})) = 0 & \mathbf{x} \in \Omega, \\
u(\mathbf{x}) = f(\mathbf{x}) & \mathbf{x} \in \partial \Omega
\end{cases}$$
(2)

might have many solutions since we do not impose structural conditions on F. For example, in case $F(\mathbf{x},u(\mathbf{x}),\nabla u(\mathbf{x}))=\lambda u$ for some $\lambda\in\mathbb{R}$ and f=0, (2) becomes an eigenvalue problem with possibly many solutions as eigenfunctions. In such cases, requiring the additional Neumann boundary condition is then natural, and (1) is not over-determined.

Next, we use our method to solve some first-order Hamilton-Jacobi equations. More precisely, to find viscosity solutions to the first-order equation

$$F(\mathbf{x}, u(\mathbf{x}), \nabla u(\mathbf{x})) = 0 \quad \mathbf{x} \in \Omega,$$

we use the vanishing viscosity procedure and consider, for $0 < \epsilon_0 \ll 1$,

$$-\epsilon_0 \Delta u(\mathbf{x}) + F(\mathbf{x}, u(\mathbf{x}), \nabla u(\mathbf{x})) = 0 \quad \mathbf{x} \in \Omega,$$

with given Cauchy boundary data. Our new method is robust in the sense that it works for general nonlinearity $F(\mathbf{x}, u, \nabla u)$ that might not be convex in ∇u . We refer the readers to [15–17] and the references therein for the theory of viscosity solutions. A weakness of our new approach in computing the viscosity solutions to Hamilton-Jacobi equations is that we need to require both Dirichlet and Neumann data of the unknown u. See [6, Remark 1.1] for some circumstances that this requirement is fulfilled. There have been many important methods to solve Hamilton-Jacobi equations in the literature. For finite difference monotone and consistent schemes of first-order equations and applications, see [18–22] for details and recent developments. If $F = F(\mathbf{x}, u, \nabla u)$ is convex in ∇u and satisfies appropriate conditions, it is possible to construct some semi-Lagrangian approximations by the discretization of the Dynamical Programming Principle associated to the problem, see [23,24] and the references therein.

The paper is organized as follows. In Section 2, we recall a Carleman estimate and two examples about inverse problems in which Problem 1 appears. In Section 3, we introduce a new iterative method based on linearization and Carleman estimates. In Section 4, we prove the convergence of our method. Some numerical results for quasilinear elliptic equations and first-order Hamilton-Jacobi equations are presented in Section 5. Concluding remarks are given in Section 6.

2. Preliminaries

In this section, we recall a Carleman estimate, which plays a key role for the proof of the convergence theorem in this paper. We then present an inverse scattering problem in which Problem (1) appears.

2.1. A Carleman estimate

In this section, we present a simple form of Carleman estimates. Carleman estimates were first employed to prove the unique continuation principle, see e.g., [25,26], and they quickly became a powerful tool in many areas of PDEs afterwards. Let \mathbf{x}_0 be a point in $\mathbb{R}^d \setminus \overline{\Omega}$ such that $r(\mathbf{x}) = |\mathbf{x} - \mathbf{x}_0| > 1$ for all $\mathbf{x} \in \Omega$. For each $\beta > 0$, define

$$\mu_{\beta}(\mathbf{x}) = r^{-\beta}(\mathbf{x}) = |\mathbf{x} - \mathbf{x}_0|^{-\beta} \quad \text{for all } \mathbf{x} \in \overline{\Omega}.$$
 (3)

We have the following lemma.

Lemma 1 (Carleman estimate). There exist positive constants β_0 , λ_0 depending only on \mathbf{x}_0 , Ω , γ , and d such that for all function $v \in C^2(\overline{\Omega})$ satisfying

$$v(\mathbf{x}) = \partial_{\nu} v(\mathbf{x}) = 0 \quad \text{for all } \mathbf{x} \in \partial\Omega,$$
 (4)

the following estimate holds true

$$\int_{\Omega} e^{2\lambda\mu_{\beta}(\mathbf{x})} |\operatorname{div}(A\nabla v)|^{2} d\mathbf{x}$$

$$\geq C\lambda \int_{\Omega} e^{2\lambda\mu_{\beta}(\mathbf{x})} |\nabla v(\mathbf{x})|^{2} d\mathbf{x} + C\lambda^{3} \int_{\Omega} e^{2\lambda\mu_{\beta}(\mathbf{x})} |v(\mathbf{x})|^{2} d\mathbf{x} \quad (5)$$

for all $\beta \geq \beta_0$ and $\lambda \geq \lambda_0$. Here, $C = C(\mathbf{x}_0, \Omega, \gamma, d, \beta) > 0$ depends only on the listed parameters.

Proof. Lemma 1 is a direct consequence of [27, Lemma 5]. Let $0 < R_1 < 1$ and $R_3 \gg 1$ such that $\Omega \in B(\mathbf{x}_0, R_3) \setminus \overline{B(\mathbf{x}_0, R_1)}$. Here, $B(\mathbf{x}_0, s) = \{\mathbf{y} \in \mathbb{R}^d : |\mathbf{y} - \mathbf{x}_0| < s\}$ for s > 0. Extend v to the whole \mathbb{R}^d such that $v(\mathbf{x}) = 0$ for all $\mathbf{x} \in \mathbb{R}^d \setminus \Omega$. Using a change of variable $\mathbf{x} \mapsto \mathbf{x} - \mathbf{x}_0$ and [27, Lemma 5], there exists a number $\beta_0 \ge 1$ depending on γ , R_1 and R_3 such that for all $\beta \ge \beta_0$ and $|\lambda| \ge 2R_3^{-\beta}$, we have

$$\int_{B(\mathbf{x}_{0},R_{3})\backslash\overline{B(\mathbf{x}_{0},R_{1})}} r(\mathbf{x})^{\beta+2} e^{2\lambda r(\mathbf{x})^{-\beta}} |\operatorname{div}(A\nabla v)|^{2} d\mathbf{x}$$

$$\geq C \int_{B(\mathbf{x}_{0},R_{3})\backslash\overline{B(\mathbf{x}_{0},R_{1})}} e^{2\lambda r^{-\beta}(\mathbf{x})} |\lambda| \beta \left(\beta^{3} \lambda^{2} r^{-2\beta-2}(\mathbf{x})|v|^{2} + |\nabla v|^{2}\right) d\mathbf{x}$$

$$- C \int_{\partial(B(\mathbf{x}_{0},R_{3})\backslash\overline{B(\mathbf{x}_{0},R_{1})})} |\lambda| \beta e^{2\lambda r^{-\beta}(\mathbf{x})} (r(\mathbf{x})|\nabla v(\mathbf{x})|^{2}$$

$$+ \beta^{2} \lambda^{2} r^{-2\beta-1}(\mathbf{x})|v(\mathbf{x})|^{2}) d\sigma(\mathbf{x}) \quad (6)$$

for some constant C depending only on d and γ . Since v=0 on $\left(B(\mathbf{x}_0,R_3)\setminus\overline{B(\mathbf{x}_0,R_1)}\right)\setminus\Omega$ and since $\Omega\in B(\mathbf{x}_0,R_3)\setminus\overline{B(\mathbf{x}_0,R_1)}$, allowing C to depend on β and Ω , we deduce the Carleman estimate (5) from (6). \square

An alternative way to obtain (5) is to apply the Carleman estimate in [28, Chapter 4, §1, Lemma 3] for general parabolic operators. The arguments to obtain (5) using [28, Chapter 4, §1, Lemma 3] are similar to that in [29, Section 3] with the Laplacian replaced by the operator $\operatorname{div}(A\nabla \cdot)$.

Remark 2. We specially draw the reader's attention to different forms of Carleman estimates for all three main kinds of differential operators (elliptic, parabolic and hyperbolic) and their applications in inverse problems and computational mathematics [30–32]. It is worth mentioning that some Carleman estimates hold true for all functions v satisfying $v|_{\partial\Omega}=0$ and $\partial_v v|_{\Gamma}=0$ where Γ is a part of $\partial\Omega$, see e.g., [6,33], which can be used to solve quasilinear elliptic PDEs with the boundary data partly given.

2.2. An inverse scattering problem

As mentioned in Section 1, Problem 1 arises from nonlinear inverse problems. We present here an important example in the context of inverse scattering problems in the frequency domain. Let $c:\mathbb{R}^d\to[1,\infty)$ be the spatially distributed dielectric constant of the medium and $[\underline{k},\overline{k}]$ be an interval of wavenumbers with $\underline{k}>0$. Since the dielectric constant of the air is 1, we set $c(\mathbf{x})=1$ for all $\mathbf{x}\in\mathbb{R}^d\setminus\Omega$. For each $k\in[\underline{k},\overline{k}]$, let $w(\mathbf{x},k),\ \mathbf{x}\in\mathbb{R}^d$, be the wave field generated by a point source at $\mathbf{x}_0\in\mathbb{R}^d\setminus\Omega$ with wavenumber k. The function w is governed by the Helmholtz equation and the Sommerfeld radiation condition

$$\begin{cases} \Delta w(\mathbf{x}, k) + k^2 c(\mathbf{x}) w(\mathbf{x}, k) = -\delta(\mathbf{x} - \mathbf{x}_0) & \mathbf{x} \in \mathbb{R}^d, \\ (\frac{\partial}{\partial |\mathbf{x}|} - ik) w(\mathbf{x}, k) = o(|\mathbf{x}|^{(1-d)/2}) & |\mathbf{x}| \to \infty. \end{cases}$$
(7)

The inverse scattering problem is formulated as follows.

Problem 2 (Inverse Scattering Problem). Compute the function c(x), $x \in \Omega$, from the measurements of

$$f_1(\mathbf{x}, k) = w(\mathbf{x}, k) \quad \text{and} \quad f_2(\mathbf{x}, k) = \partial_{\nu} w(\mathbf{x}, k)$$
 for all $\mathbf{x} \in \partial \Omega$, $k \in [\underline{k}, \overline{k}]$. (8)

The knowledge of the function c partly provides the internal structure of the domain Ω . In other words, solving the inverse scattering problem allows us to examine a domain from external measurements, which has applications in security, sonar imaging, geographical exploration, medical imaging, near-field optical microscopy, nano-optics, see,

e.g., [34] and references therein for more details. There have been many important methods to solve inverse scattering problems in the literature. Each method has its own advantages and disadvantages. A common drawback of the widely-used method based on optimization to solve inverse scattering problems is the need of a good initial guess of the true solution ϵ . We recall from [35] a method to solve the above inverse scattering problem in which such a need is relaxed. Denote by

$$z(\mathbf{x}, k) = \frac{1}{k^2} \log \left(\frac{w(\mathbf{x}, k)}{w_0(\mathbf{x}, k)} \right) \quad \text{for all } \mathbf{x} \in \Omega, k \in [\underline{k}, \overline{k}],$$

where $w_0(\mathbf{x}, k) = \frac{e^{ik|\mathbf{x}-\mathbf{x}_0|}}{4\pi|\mathbf{x}-\mathbf{x}_0|}$. Then, z satisfies

$$\Delta z(\mathbf{x},k) + k^2 |\nabla z(\mathbf{x},k)|^2 + \frac{2\nabla z(\mathbf{x},k) \cdot \nabla w_0(\mathbf{x},k)}{w_0(\mathbf{x},k)} = -c(\mathbf{x}) + 1$$

for all $\mathbf{x} \in \Omega, k \in [\underline{k}, \overline{k}]$. Let $\{\Psi_n\}_{n \geq 1}$ be the orthonormal basis of $L^2(\underline{k}, \overline{k})$ introduced in [36] and define

$$z_n(\mathbf{x}) = \int_{k}^{\overline{k}} z(\mathbf{x}, k) \Psi_n(k) dk \quad \text{for } n \ge 1, \mathbf{x} \in \Omega.$$
 (9)

We approximate

$$\upsilon(\mathbf{x},k) = \sum_{i=1}^{\infty} z_i(\mathbf{x}) \Psi_i(k) \approx \sum_{i=1}^{N} z_i(\mathbf{x}) \Psi_i(k),$$

for a suitable cut-off number $N \in \mathbb{N}$. Then, the vector $Z_N = (z_1, z_2, \dots, z_N)$ "approximately" satisfies the system

$$\sum_{i=1}^{N} s_{li} \Delta z_i(\mathbf{x}) + \sum_{i=1}^{N} a_{lij} \nabla z_i(\mathbf{x}) \cdot \nabla z_j(\mathbf{x}) + \sum_{i=1}^{N} B_{li}(\mathbf{x}) \cdot \nabla z_i(\mathbf{x}) = 0$$
 (10)

where

$$\begin{cases} s_{li} = \int\limits_{\underline{k}}^{\overline{k}} \Psi_i'(k) \Psi_l(k) dk, \\ a_{lij} = 2 \int\limits_{\underline{k}}^{\overline{k}} \left(k^2 \Psi_i(k) \Psi_j'(k) + k \Psi_i(k) \Psi_j(k) \right) \Psi_l(k) dk, \\ B_{li}(\mathbf{x}) = 2 \int\limits_{\underline{k}}^{\overline{k}} \left(\Psi_i'(k) \frac{\nabla w_0(\mathbf{x}, k)}{w_0(\mathbf{x}, k)} + \Psi_i(k) \partial_k \frac{\nabla w_0(\mathbf{x}, k)}{w_0(\mathbf{x}, k)} \right) \Psi_l(k) dk \end{cases}$$

for all $i,j,l \in \{1,\ldots,N\}$ and $\mathbf{x} \in \Omega$, see [35, Section 6] for details. The Dirichlet and Neumann boundary conditions for Z_N can be computed by the knowledges of f_1 , f_2 , and (9). Solving the system of quasilinear elliptic equations (10) with the provided Dirichlet and Neumann data is basically a goal of Problem 1. Doing so is the key step to compute c. See [35] for convexification method to compute Z_N and the procedure to obtain c from the knowledge of Z_N .

2.3. Electrical impedance tomography

We present here another potential application of our study in this paper to the 3D electrical impedance tomography (EIT) problem, so-called the 3D Calderón problem, with only a part of the Dirichlet to Neumann map is given. Let $\Omega = (-R,R)^3$ for some R>0. Let the line of source be defined as

$$L_{\rm sc} = \{ \mathbf{x}_{\alpha} = (\alpha, 0, -R) : |\alpha| \le R \} \subset \partial \Omega.$$

For each $\alpha\in[-R,R]$, let $\mathbf{x}_{\alpha}=(\alpha,0,-R)\in L_{\mathrm{sc}}$ and $w=w(\mathbf{x},\mathbf{x}_{\alpha}),\,\mathbf{x}\in\Omega,$ be the solution to

$$\begin{cases} \operatorname{div} \left(a(\mathbf{x}) \nabla w(\mathbf{x}, \mathbf{x}_{\alpha}) \right) &= 0 & \mathbf{x} \in \Omega, \\ w(\mathbf{x}, \mathbf{x}_{\alpha}) &= f_{1}(\mathbf{x}, \mathbf{x}_{\alpha}) & \mathbf{x} \in \partial \Omega. \end{cases}$$
(11)

Here, $f_1(\mathbf{x}, \mathbf{x}_a) > 0$ is a smooth approximation of the Dirac delta $\delta_0(\mathbf{x} - \mathbf{x}_a)$. In EIT, $f_1(\mathbf{x}, \mathbf{x}_a)$ represents the boundary electric voltage. The EIT problem is formulated as follows.

Problem 3 (Electrical impedance tomography). Determine the electric conductivity $a(\mathbf{x})$, $\mathbf{x} \in \Omega$, from the boundary measurement of the electric current $f_2(\mathbf{x},\mathbf{x}_a) = \partial_{\nu} w(\mathbf{x},\mathbf{x}_a)$ for all $\mathbf{x} \in \partial \Omega$, $\mathbf{x}_a \in L_{\mathrm{SC}}$.

Remark 3. Problem 3 only requests the data generated by the source moving on $L_{\rm sc}$. The dimension of this set of data is 3, including 1 dimension of the orbit $L_{\rm sc}$ of the source and 2 dimensions of the measurement surface $\partial\Omega$. This feature makes Problem 3 not over-determined because our goal is to reconstruct a 3D function a. This is unlike most of the works studying the EIT problem that request the whole Dirichlet to Neumann map $\Gamma: H^{1/2}(\partial\Omega) \to H^{-1/2}(\partial\Omega)$. Since $H^{1/2}(\partial\Omega)$, the domain of Γ , has uncountably infinity dimensions, the data requested by the Dirichlet to Neumann map is highly over-determined.

The EIT problem arises from bio-medical imaging; especially, in detecting early cancerous tumors in living tissues without operation. Most publications for the EIT problem studied the question how to reconstruct the electric conductivity $a(\mathbf{x})$, $\mathbf{x} \in \Omega$ for some domain Ω , from the Dirichlet to Neumann or the Neumann to Dirichlet map. We refer the reader to [37-40] for some well-known uniqueness results of the EIT problem. We list here a few publications for some effective approaches to numerically solve the EIT problem: the D-bar method [41-43], the methods based on optimization [44,45] and the convexification method [46]. Although effective, these methods have drawbacks. Firstly, the Dbar method is designed only for 2D. Secondly, the methods based on optimization request good initial guess of the true solution. And finally, the convexification method is time consuming. Naturally, a new computational method should be studied in this direction. Our potential method to solve the 3D EIT problem is to reduce this inverse problem to a problem of the form (1). Introduce the change of variable

$$z(\mathbf{x}, \mathbf{x}_{\alpha}) = \log \left(\sqrt{a(\mathbf{x})} w(\mathbf{x}, \mathbf{x}_{\alpha}) \right) \quad \text{for all } \mathbf{x} \in \Omega, \mathbf{x}_{\alpha} \in L_{\text{sc}}.$$
 (12)

Let $\{\Psi_n\}_{n=1}^{\infty}$ be the orthonormal basis of $L^2(-R,R)$ first introduced in [36]. Like in Section 2.2, we approximate the function $z(\mathbf{x},\mathbf{x}_{\alpha})$ as

$$z(\mathbf{x}, \mathbf{x}_{\alpha}) = \sum_{n=1}^{\infty} z_n(\mathbf{x}) \Psi_n(\alpha) \simeq \sum_{n=1}^{N} z_n(\mathbf{x}) \Psi_n(\alpha)$$
 (13)

for all $\mathbf{x} \in \Omega$, $\mathbf{x}_{\alpha} \in L_{sc}$, for some cut-off number N where

$$z_n(\mathbf{x}) = \int_{-R}^{R} z(\mathbf{x}, \mathbf{x}_{\alpha}) \Psi_n(\alpha) d\alpha$$
 (14)

for all $n \ge 1$. We choose N such that the approximation in (13) "numerically" holds for all $\mathbf{x} \in \partial \Omega$ where the data are known. Then, it is not hard to verify, see [46], that the vector $Z_N = (z_1, \dots, z_N)$ satisfies the system

$$\sum_{n=1}^{N} s_{mn} \Delta z_n(\mathbf{x}) + \sum_{n,l=1}^{N} a_{mnl} \nabla z_n(\mathbf{x}) \cdot \nabla z_l(\mathbf{x}) = 0 \quad \text{for all } \mathbf{x} \in \Omega,$$
 (15)

for each $m \in \{1, ..., N\}$, where

$$s_{mn} = \int_{-R}^{R} \Psi'_{n}(\alpha) \Psi_{m}(\alpha) d\alpha,$$

$$a_{mnl} = 2 \int^{R} \Psi_{n}(\alpha) \Psi'_{l}(\alpha) \Psi_{m}(\alpha) d\alpha.$$

The Dirichlet and Neumann boundary conditions for Z_N can be computed by the knowledges of the Dirichlet condition f_1 , the given Neumann data f_2 , (12) and (14). Solving the system of quasilinear elliptic

equations (15) with the provided Dirichlet and Neumann data is basically a goal of Problem 1. We refer the reader to [46] the step of computing a from the knowledge of the vector Z_N .

The discussion above for the inverse scattering problem and the EIT problem motivates us to study Problem 1. Since these inverse problems are out of the scope of this paper, we only mention them here to explain the significance of Problem 1. In future works, we will use our solver for Problem 1 to solve these two important inverse problems.

3. The iteration and linearization approach for Problem 1

Our approach to solve (1) is based on linearization and iteration. Assume that the solution u^* to (1) is in the space $H^p(\Omega)$ for some $p > \lfloor d/2 \rfloor + 2$ where $\lfloor d/2 \rfloor$ is the smallest integer that is greater than d/2. Define the set of admissible solutions

$$W = \left\{ \varphi \in H^p(\Omega) : \varphi|_{\partial\Omega} = f, \partial_{\nu} \varphi|_{\partial\Omega} = g \right\}. \tag{16}$$

Then, the assumption in Problem 1 implies that $W \neq \emptyset$, and $u^* \in W$. We now construct a sequence $\{u_n\}_{n \geq 0}$ that converges to the solution u^* to (1). Take a function $u_0 \in W$. Assume by induction that we have the knowledge of u_n for some $n \geq 0$. We find u_{n+1} as follows. Assume that $u^* = u_n + h$ for some $h \in H_0$ where

$$H_0 = \{ \varphi \in H^p(\Omega) : \varphi|_{\partial\Omega} = 0, \partial_{\nu} \varphi|_{\partial\Omega} = 0 \}.$$

Plugging $u^* = u_n + h$ into (1), we have

$$-\operatorname{div}(A(\mathbf{x})\nabla(u_n+h)(\mathbf{x})) + F(\mathbf{x}, u_n(\mathbf{x}) + h(\mathbf{x}), \nabla u_n(\mathbf{x}) + \nabla h(\mathbf{x})) = 0$$
(17)

for all $\mathbf{x} \in \Omega$. Heuristically, we assume at this moment that h is small, that is, $\|h\|_{C^1(\Omega)} \ll 1$.

Remark 4. The temporary assumption $\|h\|_{C^1(\Omega)} \ll 1$ is imposed for the suggestion in establishing a numerical scheme to find u_{n+1} while this condition is completely relaxed in the proof of the convergence theorem.

By Taylor's expansion, we approximate (17) as

$$-\operatorname{div}(A\nabla u_n) - \operatorname{div}(A\nabla h) + F(\mathbf{x}, u_n(\mathbf{x}), \nabla u_n(\mathbf{x})) + D\mathcal{F}(u_n)h = 0$$
(18)

for all $x \in \Omega$ where

$$D\mathcal{F}(v)h = F_s(\mathbf{x}, v(\mathbf{x}), \nabla v(\mathbf{x}))h + \nabla_{\mathbf{n}}F(\mathbf{x}, v(\mathbf{x}), \nabla v(\mathbf{x})) \cdot \nabla h(\mathbf{x})$$

for all $v \in H^p(\Omega)$. Here, F_s and $\nabla_{\mathbf{p}} F$ are the partial derivative of F with respect to its second variable and its gradient vector with respect to the third variable, respectively.

The next step is to compute a function $h \in H_0$ satisfying (18). Since there is no guarantee for the existence of such a function h, we only compute a "best fit" function h by the Carleman-based quasi-reversibility method described below. For each $v \in H^p(\Omega)$, $\lambda > 1$, $\beta > 0$ and $\eta > 0$, define the functional $J_v^{\lambda,\beta,\eta}: H_0 \to \mathbb{R}$ as

$$\begin{split} J_{v}^{\lambda,\beta,\eta}(\varphi) &= \int\limits_{\Omega} e^{2\lambda\mu_{\beta}(\mathbf{x})} \bigg| - \operatorname{div}(A\nabla\varphi) - \operatorname{div}(A\nabla\upsilon) + F(\mathbf{x},\upsilon(\mathbf{x}),\nabla\upsilon(\mathbf{x})) \\ &+ DF(\upsilon)\varphi \bigg|^{2} d\mathbf{x} + \eta \|\upsilon + \varphi\|_{H^{p}(\Omega)}^{2}. \end{split}$$

Here, the function μ_{β} is defined in (3) and $\eta \| v + \varphi \|_{H^p(\Omega)}^2$ is a regularization term.

Proposition 1. For all $\lambda > 1, \beta > 0$ and $\eta > 0$, for each $v \in H^p(\Omega)$, the functional $J_v^{\lambda,\beta,\eta}: H_0 \to H_0$ has a unique minimizer.

Proof. It is obvious that $J_v^{\lambda,\beta,\eta}$ is coercive and weakly lower semicontinuous. Thus, it has a minimizer in H_0 . The uniqueness of the minimizer can be deduced from the strict convexity of $J_v^{\lambda,\beta,\eta}$ in H_0 . \square

For each $n \ge 0$, thanks for Proposition 1, we can minimize $J_{u_n}^{\lambda,\beta,\eta}(\varphi)$ on H_0 . The unique minimizer is the desired function h. We then set

$$u_{n+1} = u_n + h. (19)$$

The construction of the sequence $\{u_n\}_{n\geq 0}$ above is summarized in Algorithm 1. We will prove that the sequence $\{u_n\}_{n\geq 0}$ converges to u^* in Section 4 as $n\to\infty$ and $\eta\to 0$. The presence of the Carleman weight $e^{2\lambda\mu_\beta(\mathbf{x})}$ is a key point for us to prove this convergence result.

Algorithm 1 The procedure to compute the numerical solution to (1).

- 1: Choose a threshold number $0 < \kappa_0 \ll 1$. Choose an arbitrary initial solution $u_0 \in W$.
- 2: Set n = 0
- 3: Solve the linear equation (18) for a function $h \in H_0$ by minimizing $J_{u_n}^{\lambda,\beta,\eta}(\varphi)$ on H_0 . Set $u_{n+1}=u_n+h$.
- 4: **if** $\|u_{n+1} u_n\|_{L^2(\Omega)} > \kappa_0$ **then**
- 5: Replace n by n + 1.
- 6: Go back to Step 3.
- 7: else
- 8: Set the computed solution $u_{comp} = u_{n+1}$.
- 9: end if

4. The convergence analysis

In this section, we prove that the sequence $\{u_n\}_{n\geq 0}$ generated by Algorithm 1 converges to the solution u^* to (1). The following result is the main theorem in this paper.

Theorem 1. Assume that $||F||_{C^2(\Omega,\mathbb{R},\mathbb{R}^d)}$ is a finite number. Assume further that (1) has a unique solution $u^* \in W$. Let $\{u_n\}_{n \geq 0}$ be the sequence generated by Algorithm 1, where $u_0 \in W$ is chosen arbitrarily. Then, there exist $\lambda_0 > 0$ and $\theta \in (0,1)$ such that, for all $\lambda > \lambda_0$,

$$\|u_{n+1} - u^*\|_{\lambda,\mu,\beta}^2 \le \theta^{n+1} \|u_0 - u^*\|_{\lambda,\mu,\beta}^2 + \eta \theta \frac{1 - \theta^{n+1}}{1 - \theta} \|u^*\|_{H^p(\Omega)}^2. \tag{20}$$

Here,

$$\|v\|_{\lambda,\mu,\beta} = \left[\int\limits_{\Omega} e^{2\lambda\mu_{\beta}(\mathbf{x})} \left(|v|^2 + |\nabla v|^2\right) d\mathbf{x}\right]^{\frac{1}{2}} \quad \textit{for all } v \in H^1(\Omega).$$

Proof. Fix $n \ge 0$. Let $h = u_{n+1} - u_n$. Due to Step 3 in Algorithm 1, h is the minimizer of $J_{u_n}^{\lambda,\beta,\eta}$. By the variational principle, we have

$$\int_{\Omega} e^{2\lambda\mu_{\beta}(\mathbf{x})} \left(-\operatorname{div}(A\nabla h) - \operatorname{div}(A\nabla u_n) + F(\mathbf{x}, u_n, \nabla u_n) + D\mathcal{F}(u_n)h \right)$$

$$\left(-\operatorname{div}(A\nabla \varphi) + D\mathcal{F}(u_n)\varphi \right) d\mathbf{x} + \eta \langle u_n + h, \varphi \rangle_{H^{p}(\Omega)} = 0 \quad (21)$$

for all $\varphi \in H_0$. Since $u_{n+1} = u_n + h$, we can rewrite (21) as

$$\begin{split} \int\limits_{\Omega} e^{2\lambda\mu_{\beta}(\mathbf{x})} \Big(-\operatorname{div}(A\nabla u_{n+1}) + F(\mathbf{x}, u_n, \nabla u_n) + D\mathcal{F}(u_n)(u_{n+1} - u_n) \Big) \\ \Big(-\operatorname{div}(A\nabla\varphi) + D\mathcal{F}(u_n)\varphi \Big) \, d\mathbf{x} + \eta \langle u_{n+1}, \varphi \rangle_{H^p(\Omega)} = 0 \end{split} \tag{22}$$

for all $\varphi \in H_0$. As u^* is the solution to (1), we have

$$\int_{\Omega} e^{2\lambda\mu_{\beta}(\mathbf{x})} \left(-\operatorname{div}(A\nabla u^*) + F(\mathbf{x}, u^*, \nabla u^*) \right)$$

 $\left(-\operatorname{div}(A\nabla\varphi) + D\mathcal{F}(u_n)\varphi\right)d\mathbf{x} = 0 \quad (23)$

for all $\varphi \in H_0$. It follows from (22) and (23) that for all $\varphi \in H_0$

$$\int_{\Omega} e^{2\lambda\mu_{\beta}(\mathbf{x})} \Big(-\operatorname{div}(A\nabla(u_{n+1} - u^*)) + F(\mathbf{x}, u_n, \nabla u_n) - F(\mathbf{x}, u^*, \nabla u^*)$$

$$+ DF(u_n)(u_{n+1} - u_n) \Big) \Big(-\operatorname{div}(A\nabla\varphi) + DF(u_n)\varphi \Big) d\mathbf{x}$$

$$+ \eta \langle u_{n+1}, \varphi \rangle_{H^{p}(\Omega)} = 0.$$
 (24)

Take $\varphi = u_{n+1} - u^* \in H_0$. It follows from (24) that

$$\int_{\Omega} e^{2\lambda\mu_{\beta}(\mathbf{x})} \Big[|\operatorname{div}(A\nabla\varphi)|^{2} - D\mathcal{F}(u_{n})\varphi \operatorname{div}(A\nabla\varphi) - \Big(F(\mathbf{x}, u_{n}, \nabla u_{n}) - F(\mathbf{x}, u^{*}, \nabla u^{*})\Big) \operatorname{div}(A\nabla\varphi) + \Big(F(\mathbf{x}, u_{n}, \nabla u_{n}) - F(\mathbf{x}, u^{*}, \nabla u^{*})\Big) D\mathcal{F}(u_{n})\varphi - \operatorname{div}(A\nabla\varphi)D\mathcal{F}(u_{n})(u_{n+1} - u_{n}) + D\mathcal{F}(u_{n})(u_{n+1} - u_{n})D\mathcal{F}(u_{n})\varphi \Big] d\mathbf{x}$$

$$= -\eta \langle u_{n+1}, \varphi \rangle_{H^{p}(\Omega)}. \quad (25)$$

As $||F||_{C^2(\Omega,\mathbb{R},\mathbb{R}^d)} = C < +\infty$, we can estimate

 $|D\mathcal{F}(u_n)\varphi| \le C(|\varphi| + |\nabla \varphi|),$

$$|F(\mathbf{x}, u_n, \nabla u_n) - F(\mathbf{x}, u^*, \nabla u^*)| \le C(|u_n - u^*| + |\nabla (u_n - u^*)|),$$

$$\begin{split} |D\mathcal{F}(u_n)(u_{n+1}-u_n)| &= |D\mathcal{F}(u_n)(u_{n+1}-u^*+u^*-u_n)| \\ &\leq C(|u_{n+1}-u^*|+|\nabla(u_{n+1}-u^*)|) + C(|u_n-u^*|+|\nabla(u_n-u^*)|), \end{split}$$

and

$$\begin{split} &-\eta\langle u_{n+1},\varphi\rangle_{H^p(\Omega)} = -\eta\langle \varphi + u^*,\varphi\rangle_{H^p(\Omega)} \\ &= -\eta\|\varphi\|_{H^p(\Omega)}^2 - \eta\langle u^*,\varphi\rangle_{H^p(\Omega)} \leq \frac{\eta}{2}\|u^*\|_{H^p(\Omega)}^2. \end{split}$$

These estimates, together with the inequality $|ab| \le 4a^2 + b^2/8$, imply

$$\int_{\Omega} e^{2\lambda\mu_{\beta}(\mathbf{x})} |\operatorname{div}(A\nabla\varphi)|^{2} d\mathbf{x} \leq C \left[\int_{\Omega} e^{2\lambda\mu_{\beta}(\mathbf{x})} (|\varphi|^{2} + |\nabla\varphi|^{2}) d\mathbf{x} \right]
+ \int_{\Omega} e^{2\lambda\mu_{\beta}(\mathbf{x})} (|u_{n} - u^{*}|^{2} + |\nabla(u_{n} - u^{*})|^{2}) d\mathbf{x} + \frac{\eta}{2} ||u^{*}||_{H^{p}(\Omega)}^{2}.$$
(26)

Applying the Carleman estimate (5) for the function φ , we have

$$\int_{\Omega} e^{2\lambda\mu_{\beta}(\mathbf{x})} |\operatorname{div}(A\nabla\varphi)|^{2} d\mathbf{x}$$

$$\geq C\lambda \int_{\Omega} e^{2\lambda\mu_{\beta}(\mathbf{x})} |\nabla\varphi(\mathbf{x})|^{2} d\mathbf{x} + C\lambda^{3} \int_{\Omega} e^{2\lambda\mu_{\beta}(\mathbf{x})} |\varphi(\mathbf{x})|^{2} d\mathbf{x}.$$
(27)

Combining (26) and (27), we have

$$\begin{split} \lambda \int_{\Omega} e^{2\lambda\mu_{\beta}(\mathbf{x})} |\nabla \varphi(\mathbf{x})|^{2} d\mathbf{x} + \lambda^{3} \int_{\Omega} e^{2\lambda\mu_{\beta}(\mathbf{x})} |\varphi(\mathbf{x})|^{2} d\mathbf{x} \\ \leq C \Big[\int_{\Omega} e^{2\lambda\mu_{\beta}(\mathbf{x})} (|\varphi|^{2} + |\nabla \varphi|^{2}) d\mathbf{x} + \int_{\Omega} e^{2\lambda\mu_{\beta}(\mathbf{x})} (|u_{n} - u^{*}|^{2} + |\nabla (u_{n} - u^{*})|^{2}) d\mathbf{x} \Big] \\ + \frac{\eta}{2} ||u^{*}||_{H^{p}(\Omega)}^{2}. \end{split} \tag{28}$$

Letting λ be sufficiently large, we can simplify (28) as

$$\lambda \int_{\Omega} e^{2\lambda\mu_{\beta}(\mathbf{x})} (|\varphi|^{2} + |\nabla\varphi|^{2}) d\mathbf{x} \le C \int_{\Omega} e^{2\lambda\mu_{\beta}(\mathbf{x})} (|u_{n} - u^{*}|^{2} + |\nabla(u_{n} - u^{*})|^{2}) d\mathbf{x} + \frac{\eta}{2} ||u^{*}||_{H^{p}(\Omega)}^{2}.$$
(29)

Recall that $\varphi = u_{n+1} - u^*$. We get from (29) that

$$\|u_{n+1} - u^*\|_{\lambda,\mu,\beta}^2 \le \frac{C}{\lambda} \|u_n - u^*\|_{\lambda,\mu,\beta}^2 + \frac{\eta}{2\lambda} \|u^*\|_{H^p(\Omega)}^2.$$
 (30)

Applying (30) for n-1 and denoting $\theta = C/\lambda \in (0,1)$, we have

$$\begin{split} \|u_{n+1} - u^*\|_{\lambda,\mu,\beta}^2 &\leq \theta \left[\theta \|u_{n-1} - u^*\|_{\lambda,\mu,\beta}^2 + \eta \theta \|u^*\|_{H^p(\Omega)}^2\right] + \eta \theta \|u^*\|_{H^p(\Omega)}^2 \\ &= \theta^2 \|u_{n-1} - u^*\|_{\lambda,\mu,\beta}^2 + \eta \theta (1+\theta) \|u^*\|_{H^p(\Omega)}^2. \end{split}$$

By induction, we have

$$||u_{n+1} - u^*||_{\lambda,\mu,\beta}^2 \le \theta^{n+1} ||u_0 - u^*||_{\lambda,\mu,\beta}^2 + \eta \theta \sum_{i=0}^n \theta^n ||u^*||_{H^p(\Omega)}^2,$$
(31)

which implies (20). The proof is complete. \Box

Remark 5 (Removing the boundedness condition of F in C^2 in Theorem 1). In the case when $\|F\|_{C^2(\Omega \times \mathbb{R} \times \mathbb{R}^{d+1})} = \infty$, we need to assume that we know in advance that the true solution u^* to (1) belongs to the ball B_M of $C^1(\Omega)$ for some M>0. This assumption does not weaken the result since M can be arbitrarily large. Define the cut-off function $\chi \in C^\infty(\Omega \times \mathbb{R} \times \mathbb{R}^d)$ as

$$\chi(\mathbf{x}, s, \mathbf{p}) = \begin{cases} 1 & |s| + |\mathbf{p}| < M, \\ 0 & |s| + |\mathbf{p}| > 2M \end{cases}$$

and set $\widetilde{F} = \chi F$. Since $|u^*| + |\nabla u^*| < M$, it is obvious that u^* solves the problem

$$\begin{cases}
-\operatorname{div}(A(\mathbf{x})\nabla u(\mathbf{x})) + \widetilde{F}(\mathbf{x}, u(\mathbf{x}), \nabla u(\mathbf{x})) = 0 & \mathbf{x} \in \Omega, \\
u(\mathbf{x}) = f(\mathbf{x}) & \mathbf{x} \in \partial\Omega, \\
\partial_{-}u(\mathbf{x}) = g(\mathbf{x}) & \mathbf{x} \in \partial\Omega.
\end{cases}$$
(32)

Now, we can apply Algorithm 1 for (32) to compute u^* .

Remark 6. Theorem 1 and estimate (20) rigorously guarantee that each sequence generated by Algorithm 1 converges to u^* at the exponential rate. This fact is numerically confirmed by our numerical results in Section 5.

Remark 7. As seen in the proof of Theorem 1, the efficiency of Algorithm 1 is guaranteed by Carleman estimate (5). Therefore, we call the proposed method described in Algorithm 1 the second generation of Carleman-based numerical methods. This second generation includes the method in [2,47] in which the iteration scheme is developed based on the contraction principle and Carleman estimates. The first generation of Carleman-based numerical method was developed in [12], which is called the convexification. See [8,6,2,35] for some following up results. Like the convexification method, Algorithm 1 can be used to compute solutions to nonlinear PDEs without requesting an initial good guess. The advantage of our new method is the fast convergence rate, see Remark 6.

5. Numerical study

In this section, we present some numerical results obtained by Algorithm 1. For simplicity, we set d = 2 and $\Omega = (-1, 1)^2$. On Ω , we arrange an $N \times N$ grid points

$$G = \{(x_i = -1 + (i-1)\delta, y_i = -1 + (j-1)\delta) : 1 \le i, j \le N\}$$

where $\delta = 2/(N-1)$. In our numerical scripts, N = 80.

In Step 1 of Algorithm 1, we choose a function $u_0 \in W$. It is natural to find a function u_0 satisfying the equation obtained by removing from (1) the nonlinearity $F(\mathbf{x}, u, \nabla u)$. We apply the Carleman-based quasi-reversibility method to do so. That means, u_0 is the minimizer of

$$J_0^{\lambda,\beta,\eta}(\varphi) = \int_{\Omega} e^{\lambda\mu_{\beta}(\mathbf{x})} |\operatorname{div}(A\nabla\varphi)|^2 d\mathbf{x} + \eta \|\varphi\|_{H^2(\Omega)}^2$$
(33)

subject to the boundary conditions in (39). To simplify the efforts in implementation, the norm in the regularization term is the $H^2(\Omega)$ -norm rather than the $H^p(\Omega)$ -norm. This change does not affect the performance of Algorithm 1. Algorithm 1 still provides satisfactory solutions to (1).

Remark 8. We employ the Carleman-based quasi-reversibility method to find u_0 for the consistency to Step 3 of Algorithm 1. Since $u_0 \in W$ can be chosen arbitrarily, one can use the quasi-reversibility method without the presence of the Carleman weight function $e^{\lambda\mu_{\beta}(\mathbf{x})}$. In our computation for all numerical examples below, $\lambda=4$, $\beta=10$ and $\mathbf{x}_0=(-4,0)$. The regularized parameter is $\eta=10^{-4}$. The threshold number $\kappa_0=10^{-6}$.

We minimize $J_0^{\lambda,\beta,\eta}$ on H_0 by the least square MATLAB command "Isqlin". The implementation for the quasi-reversibility method to minimize more general functionals than $J_0^{\lambda,\beta,\eta}$ was described in [2, §5.3] and in [48, §5]. We do not repeat this process here. In Step 3 of Algorithm 1, given $u_n \in W$, we minimize the functional $J_{u_n}^{\lambda,\beta,\eta}$ on H_0 . Again, we refer the reader to [2, §5.3] and in [48, §5] for details in implementation. The scripts for other steps of Algorithm 1 can be written easily.

5.1. Quasilinear elliptic equations

The convexification method, first introduced in [12], was used to numerically solve quasilinear elliptic equations in [8,6,35]. Our approach here is of course different based on iteration and linearization. In particular, Step 3 in Algorithm 1 is very efficient as we only need to solve the linear equation (18) as opposed to solving directly a nonlinear quasilinear elliptic equation. In this subsection, we present two (2) numerical tests. In both tests, we choose the matrix \boldsymbol{A} to be

$$A = \begin{bmatrix} 2 & 1 \\ 1 & 2 \end{bmatrix}.$$

That means, $\operatorname{div}(A\nabla u) = 2u_{xx} + 2u_{xy} + 2u_{yy}$.

In test 1, we solve (1) when

$$F(\mathbf{x}, s, \mathbf{p}) = s + |\mathbf{p}| - (-x^2 + 2y^2 + \sqrt{4x^2 + 16y^2} - 4)$$
(34)

for all $\mathbf{x} = (x, y) \in \Omega$, $s \in \mathbb{R}$ and $\mathbf{p} \in \mathbb{R}^2$. The boundary conditions are given by

$$u(\mathbf{x}) = -x^2 + 2y^2, \quad \partial_{\nu} u(\mathbf{x}) = \langle -2x, 4y \rangle \cdot \nu$$
 (35)

for all ${\bf x}=(x,y)\in\partial\Omega.$ The true solution of (1) is the function $u_{\rm true}(x,y)=-x^2+2y^2.$

It is evident from Fig. 1 that Algorithm 1 provides out of expectation solution for test 1. The relative error $\|u_{\text{true}} - u_{\text{comp}}\|_{L^{\infty}(\Omega)} / \|u_{\text{true}}\|_{L^{\infty}(\Omega)} = 1.23 \times 10^{-5}$. One can see from Fig. 1c that Algorithm 1 converges at the third iteration

In test 2, we solve (1) when

$$F(\mathbf{x}, s, \mathbf{p}) = |\mathbf{p}| - \left[\sqrt{\left[\frac{\pi}{2} \cos\left(\frac{\pi}{2}(x+y)\right) + e^{x} \right]^{2} + \frac{\pi^{2}}{4} \cos^{2}\left(\frac{\pi}{2}(x+y)\right)} + \frac{3\pi^{2}}{2} \sin\left(\frac{\pi}{2}(x+y)\right) - 2e^{x} \right]$$
(36)

for all $\mathbf{x}=(x,y)\in\Omega,\ s\in\mathbb{R}$ and $\mathbf{p}\in\mathbb{R}^2.$ The boundary conditions are given by

$$u(\mathbf{x}) = \sin\left(\frac{\pi}{2}(x+y)\right) + e^{x},$$

$$\partial_{\nu}u(\mathbf{x}) = \left\langle\frac{\pi}{2}\cos\left(\frac{\pi}{2}(x+y)\right) + e^{x},\cos\left(\frac{\pi}{2}(x+y)\right)\right\rangle \cdot \nu$$
(37)

for all $\mathbf{x} = (x, y) \in \partial \Omega$. The true solution of (1) is the function $u_{\text{true}}(x, y) = \sin\left(\frac{\pi}{2}(x+y)\right) + e^x$.

It is evident from Fig. 2 that Algorithm 1 provides out of expectation solution for test 2. The relative error $\|u_{\text{true}} - u_{\text{comp}}\|_{L^{\infty}(\Omega)} / \|u_{\text{true}}\|_{L^{\infty}(\Omega)} = 4.19 \times 10^{-5}$. One can see from Fig. 2c that Algorithm 1 converges at the fifth iteration.

5.2. Application to first-order Hamilton-Jacobi equations

Our aim in this subsection is to solve numerically

$$F(\mathbf{x}, u, \nabla u) = 0 \quad \text{for all } \mathbf{x} \in \Omega,$$
 (38)

with the boundary conditions

$$u|_{\partial\Omega} = f$$
 and $\partial_{\nu} u|_{\partial\Omega} = g$. (39)

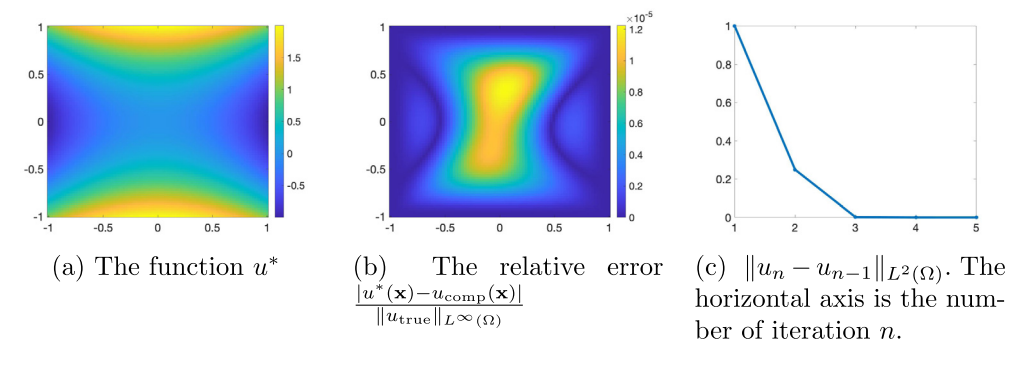


Fig. 1. Test 1. The numerical solution to (1) where *F* is given in (34) and the boundary data are given in (35).

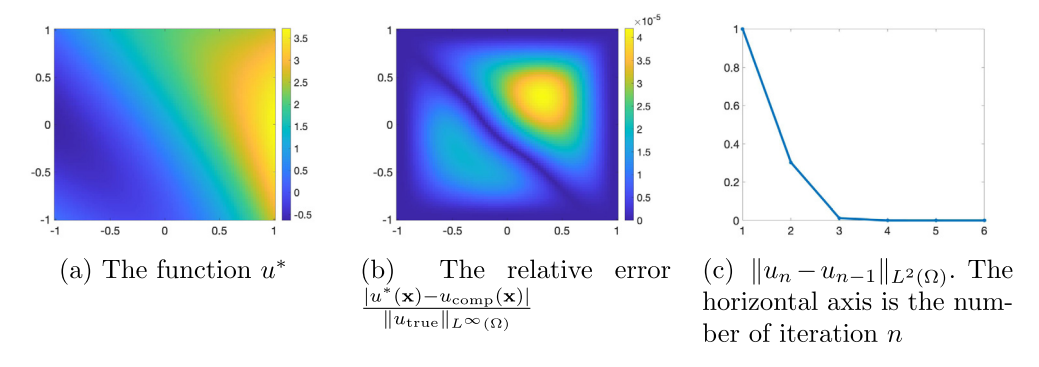


Fig. 2. Test 2. The numerical solution to (1) where F is given in (36) and the boundary data are given in (37).

Basically, we use the vanishing viscosity process to approximate solutions to (38). For $\epsilon > 0$, consider

$$-\epsilon \Delta u + F(\mathbf{x}, u, \nabla u) = 0 \quad \text{for all } \mathbf{x} \in \Omega$$
 (40)

with boundary conditions (39). Again, (40)–(39) is an over-determined boundary value problem. For $\epsilon>0$ sufficiently small, assume that (40)–(39) has a solution $u^\epsilon\in W$. Then, u^ϵ approximates u, solution to (38)–(39), quite well under some appropriate assumptions on F. In our numerical tests, we choose $\epsilon=\epsilon_0=10^{-3}$.

In this part, we provide six (6) numerical tests, in which we compute the viscosity solution to some Hamilton-Jacobi equations of the form (38) given Cauchy boundary data. That means, by applying Algorithm 1, we numerically find a function u_{comp} satisfying (40)–(39) when F, f and g are given. The verification that u^* is the correct viscosity solution can be done in a similar manner as that in [17,6].

Test 1. In this test, we solve (40)-(39) when

$$F(\mathbf{x}, s, \mathbf{p}) = s + |\mathbf{p}| + |x| - 1,$$
 (41)

for all $\mathbf{x} = (x, y) \in \Omega, s \in \mathbb{R}, \mathbf{p} \in \mathbb{R}^2$. The boundary conditions are given by

$$u(\mathbf{x}) = -|x|, \quad \partial_{\nu} u(\mathbf{x}) = \langle -\operatorname{sign}(x), 0 \rangle \cdot \nu$$
 (42)

for all $\mathbf{x}=(x,y)\in\partial\Omega$. In this case, the true solution is $u^*=-|x|$. The numerical result is displayed in Fig. 3.

It is evident from Fig. 3 that we successfully compute the solution u_{comp} . The procedure described in Algorithm 1 converges after four iterations. The relative error $\frac{\|u^*-u_{\text{comp}}\|_{L^\infty(\Omega)}}{\|u^*\|_{L^\infty(\Omega)}} = 5.33\%$.

Test 2. We find the viscosity solution to the *eikonal* equation. In this test, we solve (40)–(39) when the Hamiltonian is

$$F(\mathbf{x}, s, \mathbf{p}) = |\mathbf{p}|^2 - (1 + (1 + \text{sign}(x + y))^2)$$
(43)

for all $\mathbf{x} = (x, y) \in \Omega, s \in \mathbb{R}, \mathbf{p} \in \mathbb{R}^2$. The boundary conditions are given by

$$u(\mathbf{x}) = -|x + y| - y, \quad \partial_{\nu} u(\mathbf{x}) = (-\text{sign}(x + y), -\text{sign}(x + y) - 1) \cdot \nu$$
 (44)

for all $\mathbf{x}=(x,y)\in\partial\Omega$. The true solution is $u^*(\mathbf{x})=-|x+y|-y$. The graphs of u^* and u_{comp} are displayed in Fig. 4. The relative error $\frac{\|u^*-u_{\mathrm{comp}}\|_{L^\infty(\Omega)}}{\|u^*\|_{L^\infty(\Omega)}}=3.6\%.$

Test 3. We test the case when the Hamiltonian is not convex with respect its third variable. The Hamiltonian in this test is given by

$$F(\mathbf{x}, s, \mathbf{p}) = 20s + |p_1| - |p_2| - \left[20(-|x + 0.5| + e^{\cos(2\pi(x^2 + y^2))}) + |\operatorname{sign}(x + 0.5) + 4\pi x \sin(2\pi(x^2 + y^2))e^{\cos(2\pi(x^2 + y^2))}| - |4\pi y \sin(2\pi(x^2 + y^2))e^{\cos(2\pi(x^2 + y^2))}| \right]$$
(45)

for all $\mathbf{x}=(x,y)\in\Omega, s\in\mathbb{R}, \mathbf{p}=(p_1,p_2)\in\mathbb{R}^2.$ The boundary conditions are given by

$$u(\mathbf{x}) = -|x + 0.5| + e^{\cos(2\pi(x^2 + y^2))}$$
 for all $\mathbf{x} = (x, y) \in \partial\Omega$ (46)

and

$$\partial_{\nu} u(\mathbf{x}) = \left(-\operatorname{sign}(x+0.5) - 4\pi x \sin(2\pi (x^2 + y^2)) e^{\cos(2\pi (x^2 + y^2))}, -4\pi y \sin(2\pi (x^2 + y^2)) e^{\cos(2\pi (x^2 + y^2))} \right) \cdot \nu$$
 (47)

for all $\mathbf{x}=(x,y)\in\partial\Omega$. The true solution is $u^*(\mathbf{x})=-|x+0.5|+e^{\cos(2\pi(x^2+y^2))}$. The graphs of u^* and u_{comp} are displayed in Fig. 5. The relative error $\frac{\|u^*-u_{\mathrm{comp}}\|_{L^\infty(\Omega)}}{\|u^*\|_{L^\infty(\Omega)}}=10.65\%$. Although the relative error in this test is large, the numerical result is acceptable. In fact, we observe from Fig. 5f that $\frac{\|u^*-u_{\mathrm{comp}}\|_{L^\infty(\Omega)}}{\|u^*\|_{L^\infty(\Omega)}}$ is small almost everywhere while it is large at only two small places near the left edge of the domain.

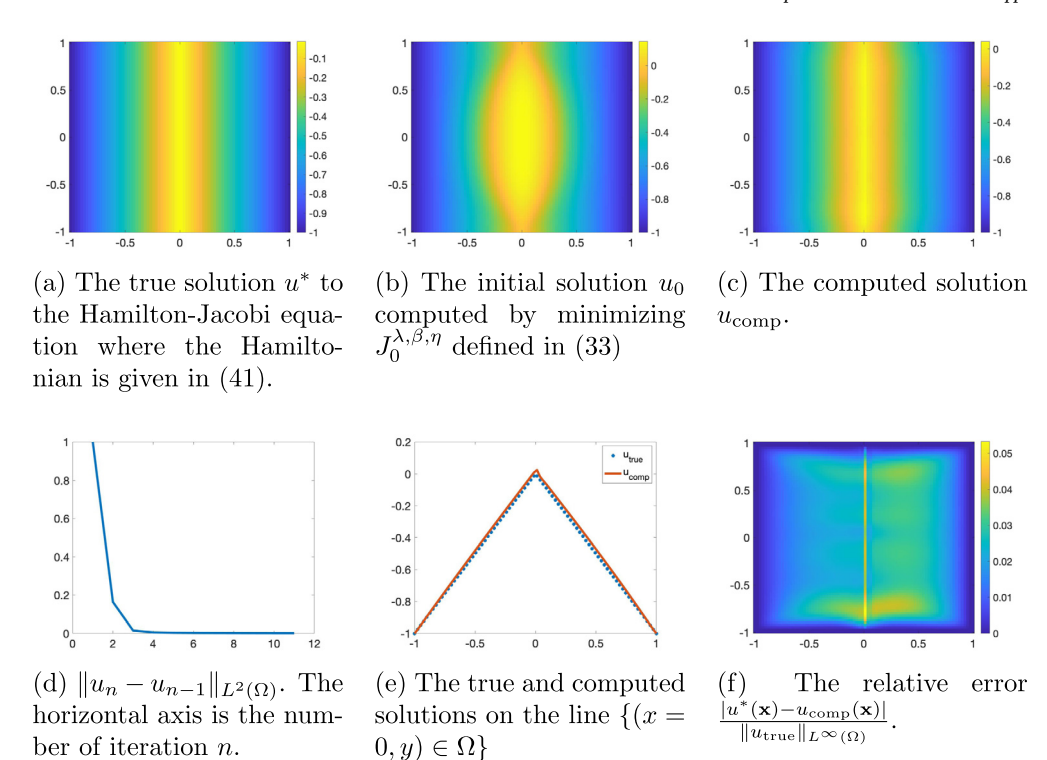


Fig. 3. Test 1. The true viscosity solution to (40)-(39) and the computed one. The Hamiltonian and the boundary conditions are given in (41)-(42).

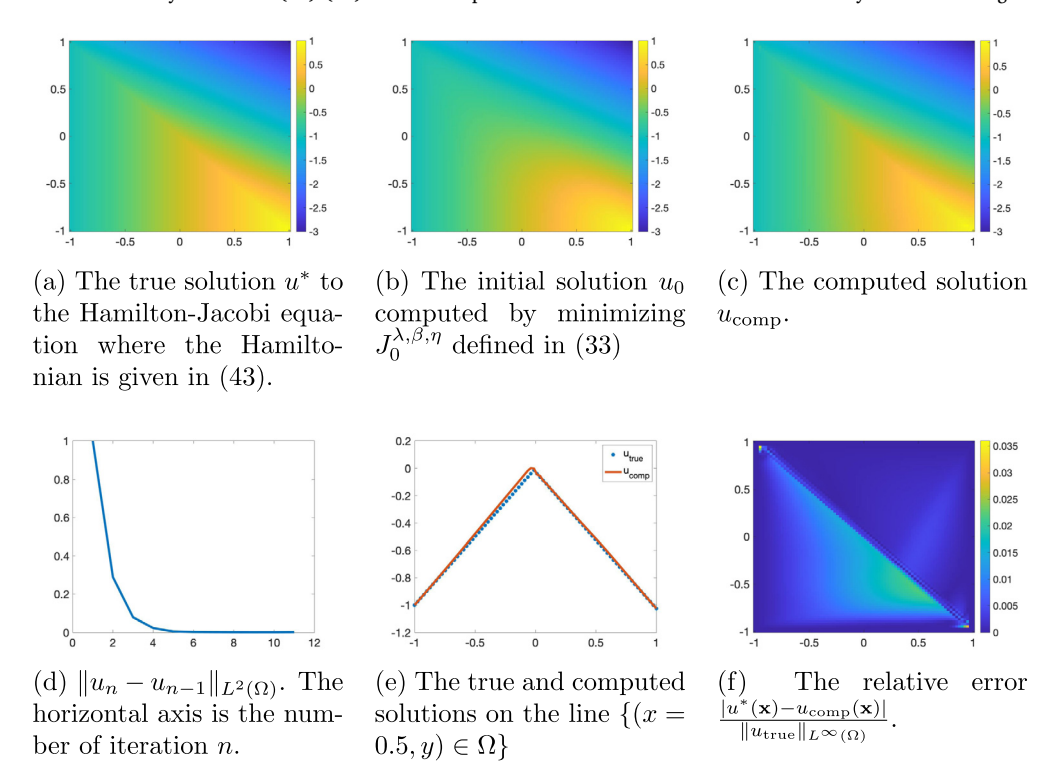


Fig. 4. Test 2. The true viscosity solution to (40)-(39) and the computed one. The Hamiltonian and the boundary conditions are given in (43)-(44).

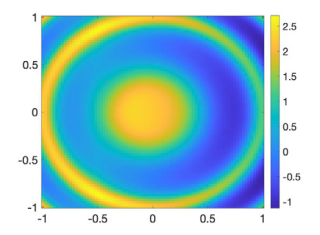
Test 4. We test the case when the Hamiltonian is not increasing in the second variable and is not convex in the third variable. The Hamiltonian in this test is given by

$$\begin{split} F(\mathbf{x}, s, \mathbf{p}) &= -40s + ||\mathbf{p}| - 10| + 40 \left(|x + y - 0.5| + \sin \left(\frac{x^2}{2} + y^2 \right) \right) \\ &- \left| \left(\left[\text{sign}(x + y - 0.5) + x \cos \left(\frac{x^2}{2} + y^2 \right) \right]^2 + \right. \end{split}$$

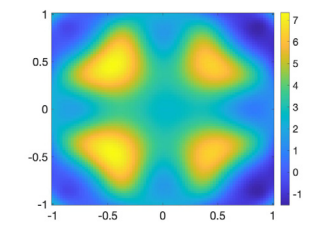
$$\left[sign(x+y-0.5) + 2y cos\left(\frac{x^2}{2} + y^2\right) \right]^2 \right)^{1/2} - 10$$
 (48)

for all $\mathbf{x} = (x, y) \in \Omega, s \in \mathbb{R}, \mathbf{p} = (p_1, p_2) \in \mathbb{R}^2$. The boundary conditions are given by

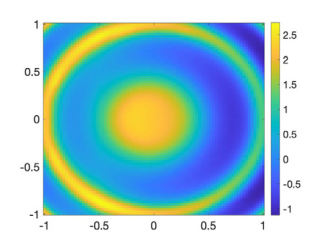
$$u(\mathbf{x}) = |x + y - 0.5| + \sin\left(\frac{x^2}{2} + y^2\right) \quad \text{for all } \mathbf{x} = (x, y) \in \partial\Omega$$
 and



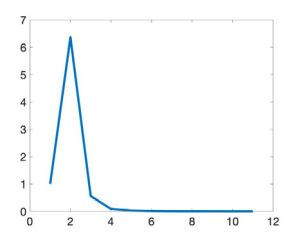
(a) The true solution u^* to the Hamilton-Jacobi equation where the Hamiltonian is given in (45).



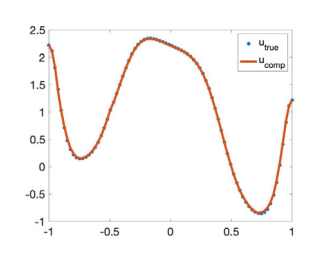
(b) The initial solution u_0 computed by minimizing $J_0^{\lambda,\beta,\eta}$ defined in (33)



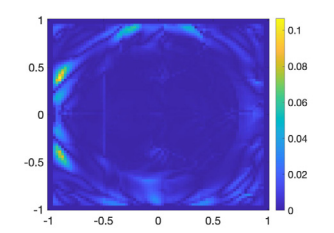
(c) The computed solution u_{comp} .



(d) $||u_n - u_{n-1}||_{L^2(\Omega)}$. The horizontal axis is the number of iteration n.



(e) The true and computed solutions on the line $\{(x = 0, y) \in \Omega\}$



(f) The relative error $\frac{|u^*(\mathbf{x}) - u_{\text{comp}}(\mathbf{x})|}{\|u_{\text{true}}\|_{L^{\infty}(\Omega)}}.$

Fig. 5. Test 3. The true viscosity solution to (40)-(39) and the computed one. The Hamiltonian and the boundary conditions are given in (45)-(47).

$$\partial_{\nu}u(\mathbf{x}) = \left(\operatorname{sign}(x+y-0.5) + x\cos\left(\frac{x^2}{2} + y^2\right),\right.$$
$$\operatorname{sign}(x+y-0.5) + 2y\cos\left(\frac{x^2}{2} + y^2\right)\right) \cdot \nu \tag{50}$$

for all $\mathbf{x}=(x,y)\in\partial\Omega$. The true solution is $u^*(\mathbf{x})=|x+y-0.5|+\sin\left(\frac{x^2}{2}+y^2\right)$. The graphs of u^* and u_{comp} are displayed in Fig. 6. The relative error $\frac{\|u^*-u_{\text{comp}}\|_{L^\infty(\Omega)}}{\|u^*\|_{L^\infty(\Omega)}}=0.95\%$.

 $\mathit{Test}\ 5.$ We solve a G-equation. The Hamiltonian in this test is given by

$$F(\mathbf{x}, s, \mathbf{p}) = 5s + |\mathbf{p}| - xp_1 + \left[5(|x - 0.5| + |y|) - x \operatorname{sign}(x - 0.5) - \sqrt{2} \right]$$
 (51)

for all $\mathbf{x} = (x, y) \in \Omega$, $s \in \mathbb{R}$, $\mathbf{p} = (p_1, p_2) \in \mathbb{R}^2$. The boundary conditions are given by

$$u(\mathbf{x}) = -|x - 0.5| - |y| \quad \text{for all } \mathbf{x} = (x, y) \in \partial\Omega$$
 (52)

and

$$\partial_{\nu}u(\mathbf{x}) = -\left(\operatorname{sign}(x - 0.5), \operatorname{sign}(y)\right) \cdot \nu \tag{53}$$

for all $\mathbf{x}=(x,y)\in\partial\Omega$. The true solution is $u^*(\mathbf{x})=-|x-0.5|-|y|$. The graphs of u^* and u_{comp} are displayed in Fig. 7. The relative error $\frac{\|u^*-u_{\mathrm{comp}}\|_{L^\infty(\Omega)}}{\|u^*\|_{L^\infty(\Omega)}}=0.98\%.$

Test 6. The Hamiltonian in this test is given by

$$F(\mathbf{x}, s, \mathbf{p}) = 20s + \min\{|\mathbf{p}|, ||\mathbf{p}| - 10| + 6\} - \left[20(-|x| + \sin(\pi(x^2 + y^2))) + \min\left\{h(x, y), |h(x, y) - 10| + 6\right\}\right]$$
(54)

for all $\mathbf{x} = (x, y) \in \Omega$, $s \in \mathbb{R}$, $\mathbf{p} = (p_1, p_2) \in \mathbb{R}^2$ where

$$h(x,y) = \sqrt{[-\text{sign}(x) + 2\pi\cos(\pi(x^2 + y^2))]^2 + [2\pi\cos(\pi(x^2 + y^2)]^2}.$$

The boundary conditions are given by

$$u(\mathbf{x}) = -|x| + \sin(\pi(x^2 + y^2)) \quad \text{for all } \mathbf{x} = (x, y) \in \partial\Omega$$
 (55)

and

$$\partial_{\nu}u(\mathbf{x}) = \left(-\operatorname{sign}(x) + 2\pi x \cos(\pi(x^2 + y^2)), 2\pi y \cos(\pi(x^2 + y^2))\right) \cdot \nu \tag{56}$$

for all $\mathbf{x} = (x,y) \in \partial \Omega$. The true solution is $u^*(\mathbf{x}) = -|x| + \sin(\pi(x^2 + y^2))$. The graphs of u^* and u_{comp} are displayed in Fig. 8. The relative error $\frac{\|u^* - u_{\text{comp}}\|_{L^\infty(\Omega)}}{\|u^*\|_{L^\infty(\Omega)}} = 4.8\%.$

Remark 9. The L^{∞} relative errors in all tests above for first-order Hamilton-Jacobi equations are compatible with $\max\{O(\sqrt{\eta}), O(\sqrt{\varepsilon_0})\} \simeq \frac{20}{3}$

6. Concluding remarks

We have developed a new globally convergent numerical method to solve over-determined boundary value problems of quasilinear elliptic equations. The key point of the method is to repeatedly solve the linearization of the given PDE by the Carleman weighted quasireversibility method (Algorithm 1). As the result, we obtain a sequence of functions converging to the solution thanks to the Carleman estimate (Lemma 1). The strength of our new method includes (1) the global convergence property and (2) the fast convergence rate, which is described in Theorem 1. Some numerical results for quasilinear elliptic equations and first-order Hamilton-Jacobi equations are presented to show the effectiveness of our method.

Acknowledgement

The works of TTL and LHN were supported in part by US Army Research Laboratory and US Army Research Office grant W911NF-19-1-0044, by NSF Grant DMS-2208159, and by funds provided by the Faculty Research Grant program at UNC Charlotte, Fund No. 111272. The work of HT is supported in part by NSF CAREER grant DMS-1843320 and a Simons Fellowship 818813.

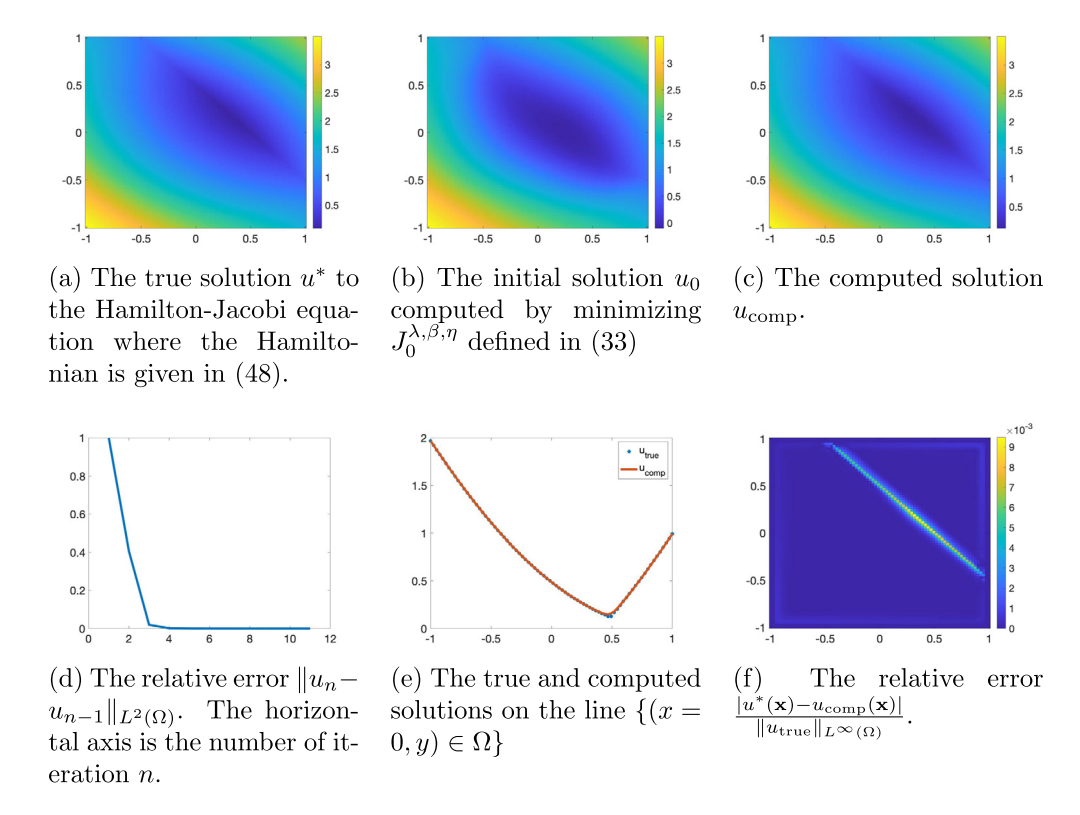


Fig. 6. Test 4. The true viscosity solution to (40)-(39) and the computed one. The Hamiltonian and the boundary conditions are given in (48)-(50).

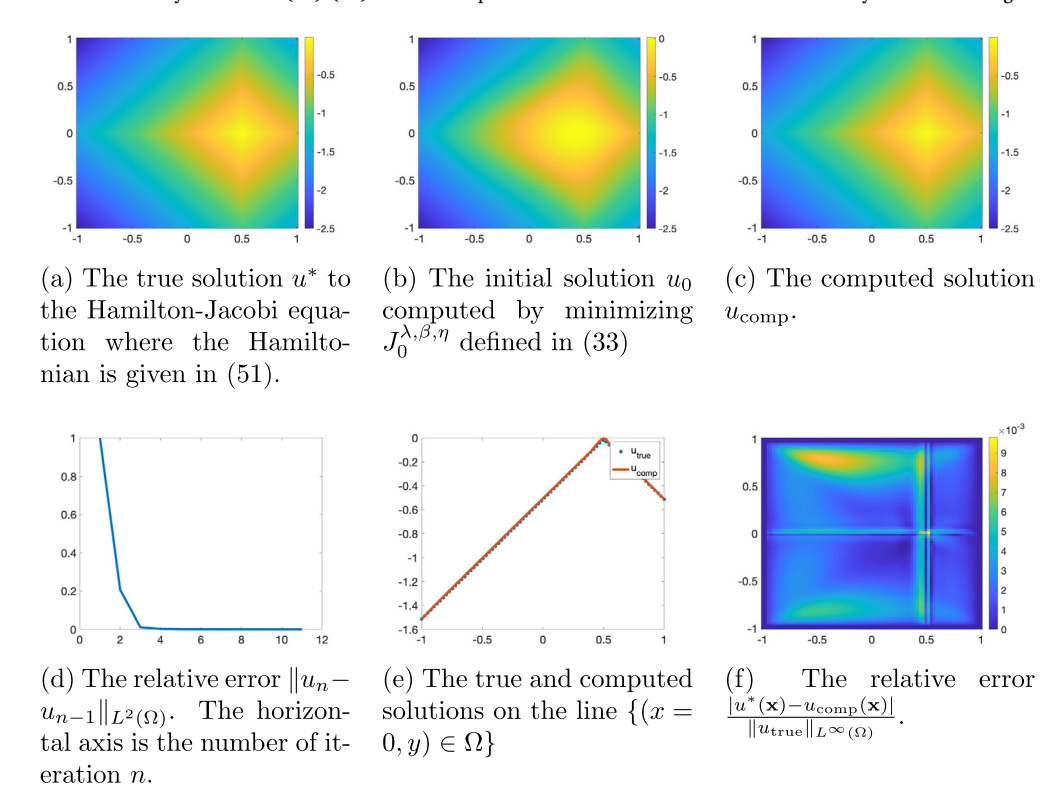


Fig. 7. Test 5. The true viscosity solution to (40)-(39) and the computed one. The Hamiltonian and the boundary conditions are given in (51)-(53).

References

- [1] V.A. Khoa, M.V. Klibanov, L.H. Nguyen, Convexification for a 3D inverse scattering problem with the moving point source, SIAM J. Imaging Sci. 13 (2) (2020) 871–904.
- [2] T.T. Le, L.H. Nguyen, A convergent numerical method to recover the initial condition of nonlinear parabolic equations from lateral Cauchy data, J. Inverse Ill-Posed Probl. (2020), https://doi.org/10.1515/jiip-2020-0028.
- [3] V.A. Khoa, G.W. Bidney, M.V. Klibanov, L.H. Nguyen, L. Nguyen, A. Sullivan, V.N. Astratov, Convexification and experimental data for a 3D inverse scattering problem with the moving point source, Inverse Probl. 36 (2020) 085007.
- [4] V.A. Khoa, G.W. Bidney, M.V. Klibanov, L.H. Nguyen, L. Nguyen, A. Sullivan, V.N. Astratov, An inverse problem of a simultaneous reconstruction of the dielectric constant and conductivity from experimental backscattering data, Inverse Probl. Sci. Eng. 29 (5) (2021) 712–735.

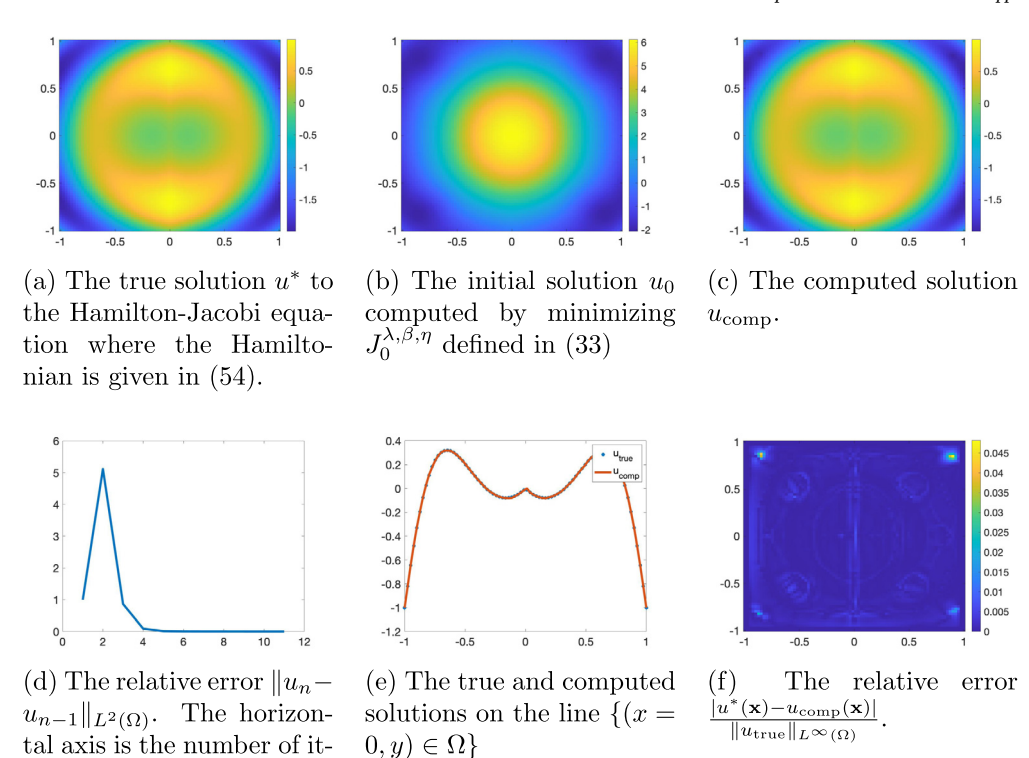


Fig. 8. Test 6. The true viscosity solution to (40)-(39) and the computed one. The Hamiltonian and the boundary conditions are given in (54)-(56).

[5] M.V. Klibanov, T.T. Le, L.H. Nguyen, A. Sullivan, L. Nguyen, Convexification-based globally convergent numerical method for a 1D coefficient inverse problem with experimental data, Inverse Probl. Imaging (2021), https://doi.org/10.3934/ipi.2021068, in press.

eration n.

- [6] M.V. Klibanov, L.H. Nguyen, H.V. Tran, Numerical viscosity solutions to Hamilton-Jacobi equations via a Carleman estimate and the convexification method, J. Comput. Phys. 451 (2022) 110828.
- [7] J.A. Scales, M.L. Smith, T.L. Fischer, Global optimization methods for multimodal inverse problems, J. Comput. Phys. 103 (1992) 258–268.
- [8] A.B. Bakushinskii, M.V. Klibanov, N.A. Koshev, Carleman weight functions for a globally convergent numerical method for ill-posed Cauchy problems for some quasilinear PDEs, Nonlinear Anal., Real World Appl. 34 (2017) 201–224.
- [9] M.V. Klibanov, Global convexity in a three-dimensional inverse acoustic problem, SIAM J. Math. Anal. 28 (1997) 1371–1388.
- [10] M.V. Klibanov, Global convexity in diffusion tomography, Nonlinear World 4 (1997) 247–265.
- [11] M.V. Klibanov, Carleman weight functions for solving ill-posed Cauchy problems for quasilinear PDEs, Inverse Probl. 31 (2015) 125007.
- [12] M.V. Klibanov, O.V. Ioussoupova, Uniform strict convexity of a cost functional for three-dimensional inverse scattering problem, SIAM J. Math. Anal. 26 (1995) 147–179
- [13] R. Lattès, J.L. Lions, The Method of Quasireversibility: Applications to Partial Differential Equations, Elsevier, New York, 1969.
- [14] M.V. Klibanov, Carleman estimates for the regularization of ill-posed Cauchy problems, Appl. Numer. Math. 94 (2015) 46–74.
- [15] M.G. Crandall, P.-L. Lions, Viscosity solutions of Hamilton-Jacobi equations, Trans. Am. Math. Soc. 277 (1) (1983) 1–42, https://doi.org/10.2307/1999343.
- [16] M.G. Crandall, L.C. Evans, P.-L. Lions, Some properties of viscosity solutions of Hamilton-Jacobi equations, Trans. Am. Math. Soc. 282 (2) (1984) 487–502, https://doi.org/10.2307/1999247.
- [17] H. Tran, Hamilton–Jacobi Equations: Theory and Applications, Graduate Studies in Mathematics, American Mathematical Society, 2021, https://books.google.com/ books?id=evs-EAAAQBAJ.
- [18] G. Barles, P.E. Souganidis, Convergence of approximation schemes for fully nonlinear second order equations, Asymptot. Anal. 4 (3) (1991) 271–283.
- [19] M.G. Crandall, P.-L. Lions, Two approximations of solutions of Hamilton-Jacobi equations, Math. Comput. 43 (167) (1984) 1–19, https://doi.org/10.2307/2007396.
- [20] S. Osher, R. Fedkiw, Level Set Methods and Dynamic Implicit Surfaces, Applied Mathematical Sciences, vol. 153, Springer-Verlag, New York, 2003, https://doi-org. ezproxy.library.wisc.edu/10.1007/b98879.
- [21] J.A. Sethian, Level Set Methods and Fast Marching Methods: Evolving Interfaces in Computational Geometry, Fluid Mechanics, Computer Vision, and Materials Science, 2nd edition, Cambridge Monographs on Applied and Computational Mathematics, vol. 3, Cambridge University Press, Cambridge, 1999.

- [22] P.E. Souganidis, Approximation schemes for viscosity solutions of Hamilton-Jacobi equations, J. Differ. Equ. 59 (1) (1985) 1–43, https://doi.org/10.1016/0022-0396(85)90136-6.
- [23] M. Falcone, R. Ferretti, Semi-Lagrangian schemes for Hamilton-Jacobi equations, discrete representation formulae and Godunov methods, J. Comput. Phys. 175 (2) (2002) 559–575, https://doi.org/10.1006/jcph.2001.6954.
- [24] M. Falcone, R. Ferretti, Semi-Lagrangian Approximation Schemes for Linear and Hamilton-Jacobi Equations, Society for Industrial and Applied Mathematics (SIAM), Philadelphia, PA, 2014.
- [25] T. Carleman, Sur les systèmes linéaires aux derivées partielles du premier ordre a deux variables, C. R. Acad. Sci. Paris 197 (1933) 471–474.
- [26] M.H. Protter, Unique continuation for elliptic equations, Trans. Am. Math. Soc. 95 (1) (1960) 81–91.
- [27] H.M. Nguyen, L.H. Nguyen, Cloaking using complementary media for the Helmholtz equation and a three spheres inequality for second order elliptic equations, Trans. Am. Math. Soc. 2 (2015) 93–112.
- [28] M.M. Lavrent'ev, V.G. Romanov, S.P. Shishat-skiĭ, Ill-Posed Problems of Mathematical Physics and Analysis, Translations of Mathematical Monographs, AMS, Providence, RI, 1986.
- [29] T.T. Le, L.H. Nguyen, T.-P. Nguyen, W. Powell, The quasi-reversibility method to numerically solve an inverse source problem for hyperbolic equations, J. Sci. Comput. 87 (2021) 90.
- [30] L. Beilina, M.V. Klibanov, Approximate Global Convergence and Adaptivity for Coefficient Inverse Problems, Springer, New York, 2012.
- [31] A.L. Bukhgeim, M.V. Klibanov, Uniqueness in the large of a class of multidimensional inverse problems, Sov. Math. Dokl. 17 (1981) 244–247.
- [32] M.V. Klibanov, J. Li, Inverse Problems and Carleman Estimates: Global Uniqueness, Global Convergence and Experimental Data, De Gruyter, 2021.
- [33] L.H. Nguyen, Q. Li, M.V. Klibanov, A convergent numerical method for a multi-frequency inverse source problem in inhomogenous media, Inverse Probl. Imaging 13 (2019) 1067–1094.
- [34] D. Colton, R. Kress, Inverse Acoustic and Electromagnetic Scattering Theory, 3rd edition, Applied Mathematical Sciences, Springer, New York, 2013.
- [35] T.T. Le, L.H. Nguyen, The gradient descent method for the convexification to solve boundary value problems of quasi-linear PDEs and a coefficient inverse problem, J. Sci. Comput. 91 (2022) 74.
- [36] M.V. Klibanov, Convexification of restricted Dirichlet to Neumann map, Inverse Illposed Probl. Ser. 25 (5) (2017) 669–685.
- [37] A.P. Calderón, On an inverse boundary value problem, in: Seminar on Numerical Analysis and Its Applications to Continuum Physics, Río de Janeiro, Soc. Brasileira de Matemática. 1980.
- [38] R.V. Kohn, M. Vogelius, Determining conductivity by boundary measurements II. Interior results, Commun. Pure Appl. Math. 38 (1985) 643–667.

- [39] A.I. Nachman, Global uniqueness for a two-dimensional inverse boundary value problem, Ann. Math. 143 (1996) 71–96.
- [40] J. Sylvester, G. Uhlmann, A global uniqueness theorem for an inverse boundary value problem, Ann. Math. 125 (1) (1987) 153–169.
- [41] K. Knudsen, M. Lassas, J.L. Mueller, S. Siltanen, Regularized D-bar method for the inverse conductivity problem, Inverse Probl. 3 (2009) 599–624.
- [42] J.L. Mueller, S. Siltanen, The D-bar method for electrical impedance tomographydemystified, Inverse Probl. 36 (2020) 093001.
- [43] E.K. Murphy, J.L. Mueller, Effect of domain shape modeling and measurement errors on the 2-D D-bar method for EIT, IEEE Trans. Med. Imaging 28 (2009) 1576–1584.
- [44] G. González, V. Kolehmainen, A. Seppänen, Isotropic and anisotropic total variation regularization in electrical impedance tomography, Comput. Math. Appl. 74 (2017) 564–576.
- [45] Z. Zhou, G. Sato dos Santos, T. Dowrick, J. Avery, Z. Sun, H. Xu, D. Holder, Comparison of total variation algorithms for electrical impedance tomography, Physiol. Meas. 36 (6) (2015) 1193.
- [46] M.V. Klibanov, J. Li, W. Zhang, Convexification of electrical impedance tomography with restricted Dirichlet-to-Neumann map data, Inverse Probl. 35 (2019) 035005.
- [47] L.H. Nguyen, M.V. Klibanov, Carleman estimates and the contraction principle for an inverse source problem for nonlinear hyperbolic equations, Inverse Probl. 38 (2022) 035009.
- [48] L.H. Nguyen, A new algorithm to determine the creation or depletion term of parabolic equations from boundary measurements, Comput. Math. Appl. 80 (2020) 2135–2149.